Use of saponin foam reinforced with colloidal particles as an application to soil remediation: Experiments in a 2D tank

Natacha Forey, Olivier Atteia, Abdelaziz Omari, Henri Bertin

Version of Record: https://www.sciencedirect.com/science/article/pii/S0169772220303508
Manuscript_0f61686e38377deee9d68221aadd1b4b

Use of saponin foam reinforced with colloidal particles as an application to soil remediation: experiments in a 2D tank

Natacha Forey[a*], Olivier Atteia[b], Abdelaziz Omari[a], Henri Bertin[a]
[a]*I2M, UMR CNRS 5295, Université de Bordeaux, Esplanade des Arts et Métiers, 33405 Talence Cedex, France*
[b]*ENSEGID, EA 4592, 1 Allée Fernand Daguin, 33607 Pessac, France*

*Corresponding author
E-mail address: natacha.forey@free.fr

Keywords: Foam, Porous medium, Colloidal particle, Light Non Aqueous Phase Liquid, 2D tank

Highlights

- A piston-like front is forming when injecting foam in a 2D-porous medium
- Oil presence disturbs foam displacement and foam front
- Solid silica particles increase foam resistance to oil induced destruction

Graphical abstract

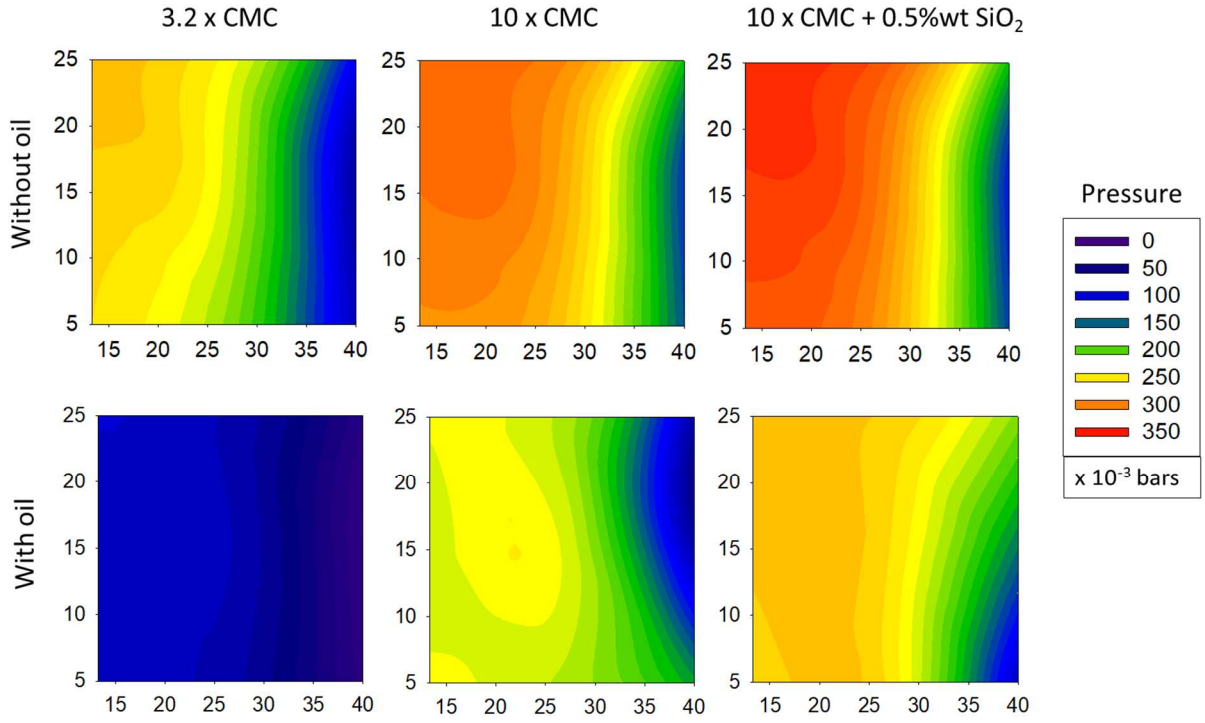

Abstract

Foam can be used to achieve environmental remediation in case of contamination caused by light non aqueous phase spills. However, when it comes in contact with oily pollutants, foam becomes weaker and its life time is greatly reduced. Such weakening can be dampened by using silica particles -together with saponin surfactant- which were shown to reinforce foam in bulk and 1D sandpack experiments. Here is addressed both foam propagation in a 2D porous media when buoyancy and gravity interfere, and foam behaviour when in contact with floating oil. Therefore, macroscopic foam displacement, and specific liquid and gas phases behaviours were

studied in a 2D-tank. A piston-like displacement was observed during foam propagation in the absence of oil, while foam liquid phase was influenced by gravity and did not propagate homogeneously on entire tank height. In the presence of oil, foam was partly destroyed, which increased the local permeability of gas and created new preferential paths for gas flow. This effect was partially avoided via a surfactant concentration increase, but solid colloidal particles turned out to be a more efficient stabilizing agent, by significantly increasing foam strength and its oil-tolerance.

1. Introduction

Remediation of Light Non Aqueous Phase Liquid (LNAPL) contaminated soils is crucial for public health and environmental issues. It can be achieved using different techniques, varying with pollution type and contamination depth, soil permeability and soil geophysical properties. Depending on the chosen treatment, remediation strategies can be *ex-situ*: the pollution is treated outside the site, and excavation is necessary. However, due to the cost of excavation, the use of *in-situ* remediation techniques is indicated. Among these techniques, surfactant flushing allows reduction of the surface tension between water and the pollutant, easing pollutant removal and solubilisation of the hydrocarbon molecules in surfactant micelles. Nevertheless, the needed amount of surfactant may be too high, and the sweeping efficiency is sometimes low, especially in heterogeneous porous media. To avoid these drawbacks, the use of aqueous foam is recommended [1].

Liquid foam is made of a gaseous phase dispersed in a continuous aqueous phase. The thin films separating gas bubbles are called lamellae and are stabilized by surfactants. These amphiphilic molecules adsorb at the gas-water interface, decrease the interfacial tension, limiting bubble coalescence and film rupture. Such a dispersion of gas in a liquid phase results in a high viscosity fluid where gravity segregation, channelling and fingering are avoided [2] and, consequently gas mobility is severely reduced [3].

Because of its high viscosity, foam can be used to block high permeability zones of a heterogeneous porous medium, thus allowing other injected fluids to access low permeability zones that are then more easily swept [4]. Foam can also serve as a tool in remediation strategy to recover floating pollutant with a good sweeping efficiency, by pushing it to a pumping well [5], or to bring oxidative chemicals to the contaminant source, where they will react with the pollutant to form non-toxic compounds [6]. It can also serve to confine a polluted area waiting for the appropriate treatment [7]. For the method that aims to recover a floating pollutant, the objective is to inject foam underneath a LNAPL layer, so as to decrease the water flow towards the pumping well in order to increase the pumping rate of the LNAPL. This may be achieved with a foam of high sweeping efficiency and high viscosity.

However, to be of optimum quality and be efficient, foam has to fulfil two requirements. The first requirement is to be of low sensitivity to buoyancy, and such a sensitivity is related to foam structure, its quality and its viscosity. The second requirement is foam formulation, which should be robust enough to resist oil-induced de-foaming effect. Indeed, foam is destabilized by oil both in bulk and in porous medium [8]. This process has been extensively studied, and is mainly governed by the destabilization of the foam-oil interface, called pseudo-emulsion film [9]. Therefore, additional foam reinforcement is necessary.

In that respect, it was concluded from previous experiments performed in 1D sandpack columns, that the addition of native silica colloidal particles does effectively increase foam resistance against oil-induced coalescence [10]. By irreversibly adsorbing at the gas-water interface, silica particles increase the interfacial elasticity [11] and steric repulsion, thus decreasing the film drainage rate [12]. Such a solid barrier in turn increases the strength of the pseudo-emulsion film, and reinforces foam resistance against oil. To get a maximum foam

stability, depending on the system considered, silica particles are sometimes surface-treated to adjust their degree of hydrophobicity to an optimum value [13]. Silica particles also have the benefit of being natural products commonly used in food or medical applications [14].

To study buoyancy effects, and because they were negligible in 1D sandpack experiments, the focus is here placed on foam displacement in a 2D-vertical porous medium to mimic the application conditions. The objectives of the experiments are to characterize foam behaviour in a vertical porous medium, and to investigate how the liquid and gas phases of foam typically flow. Our work relies on the work of a few authors who have investigated foam propagation in 2D-tanks for soil remediation [5,15,16]. Although, some authors studied foam reinforced with solid colloidal particles in 2D-tanks, the performance of such Pickering-like foams was evaluated for Enhanced Oil Recovery (EOR) applications [17,18]. And they used quite different operating conditions and surfactants, injecting foam only in small containers where buoyancy was of less relevance [17].

Moreover, given the environmental application, foam formulation should in fact, be as friendly as possible. So saponin, a biodegradable surfactant was chosen for foam generation in the present study. It is a plant-based surfactant with interesting foaming properties [19], and has been successfully used for the removal of heavy metals and mixed contaminants via desorption and solubilisation of contaminants [20]. It has also been used in synergy with solid colloidal particles for food-grade foam stabilization

So, the main goal of this study is to explore the impact of foam formulation on individual phase displacement in a 2D vertical porous medium, in the absence and in the presence of oil. This was first achieved through the analysis of several macroscopic parameters: sequential imaging, pressure field and water saturation (S_w). In these first experiments, no oil was present since the objective was to determine how buoyancy modifies foam behaviour when surfactant and colloidal particles concentrations vary. Later, foam behaviour was studied in the presence of a top layer at residual oil saturation (S_{or}) to mimic a real operating situation and to study how solid particles affect foam resistance against oil.

2. Experimental

2.1. Chemicals

The surfactant used was saponin (non-ionic, Sigma-Aldrich, France) with a critical micelle concentration (CMC) of 0.062%wt. Native silica particles (LUDOX® TM-50, Sigma-Aldrich, France) have a nominal size of 30 nm, as measured by Orts-Gils et *al.* [21], and were used as received. As native solid particles suspensions were in aggregated state, they were systematically sonicated 10 minutes by means of an ultrasonic bath equipment (FisherbrandTM Elmasonic, Fisher Scientific France). Nitrogen of high purity (purity > 99.999%) was supplied by Air Liquide (France). It was used to control the level of purity of the gas, and to avoid potential oxidation of the chemicals by O_2. The pollutant oil used was MACRON 1821 F-4 (Houghton, US), a refined cutting oil with a density of 0.818 at T = 20°C. When needed, fluorescein sodium salt (Sigma-Aldrich, France) was used as an inert dying agent.

2. 2. Preparation of foaming solutions and porous medium

All foaming solutions were prepared using tap water which ionic strength was less than 10^{-2} M. The surfactant (saponin) was dissolved in water at the desired concentration, expressed as a multiple of critical micelle concentration (×CMC), and steered at 400 rpm for at least twenty minutes.

To prepare aqueous solutions containing solid particles, silica particles were first mechanically dispersed in a given amount of water, and vigorously sonicated for 10 minutes in

an ultrasonic bath. In parallel, the surfactant was dissolved in the same amount of water before blending the two solutions in convenient volume proportions.

A 40 cm long, 3 cm wide, and 30 cm high tank, built with 3 cm thick transparent PMMA sides was used as a container. It was then packed with clean sand purchased from Cantillana (Cantillana, France), with a D_{50} grain size of 279 µm.

2.3. Experimental set-up

The experimental setup is presented in Figure 1. To generate foam, aqueous foaming solution and nitrogen were simultaneously co-injected into the 2-D porous medium.

To inject aqueous foaming solutions, two piston pumps PHD ULTRA™ (Harvard Apparatus, US) were used with two syringes. To inject nitrogen, two mass flow meters (EL-FLOW®, Bronkhorst® France) were used in nominal conditions. Both gas and the foaming solution were injected at controlled flow rates.

Ten digital pressure sensors (Idroscan from AEP transducers, Italy) regularly distributed across the porous medium were used to measure the absolute pressure. The upper two taps situated at the tank sides were connected via a differential pressure transducer (Rosemount 2051 Coplanar™, Emerson, France) and a camera (Panasonic Lumix DMC-TZ70) was used to take pictures of the tank during foam propagation. Finally, the effluents were weighed over time and a mass balance calculated.

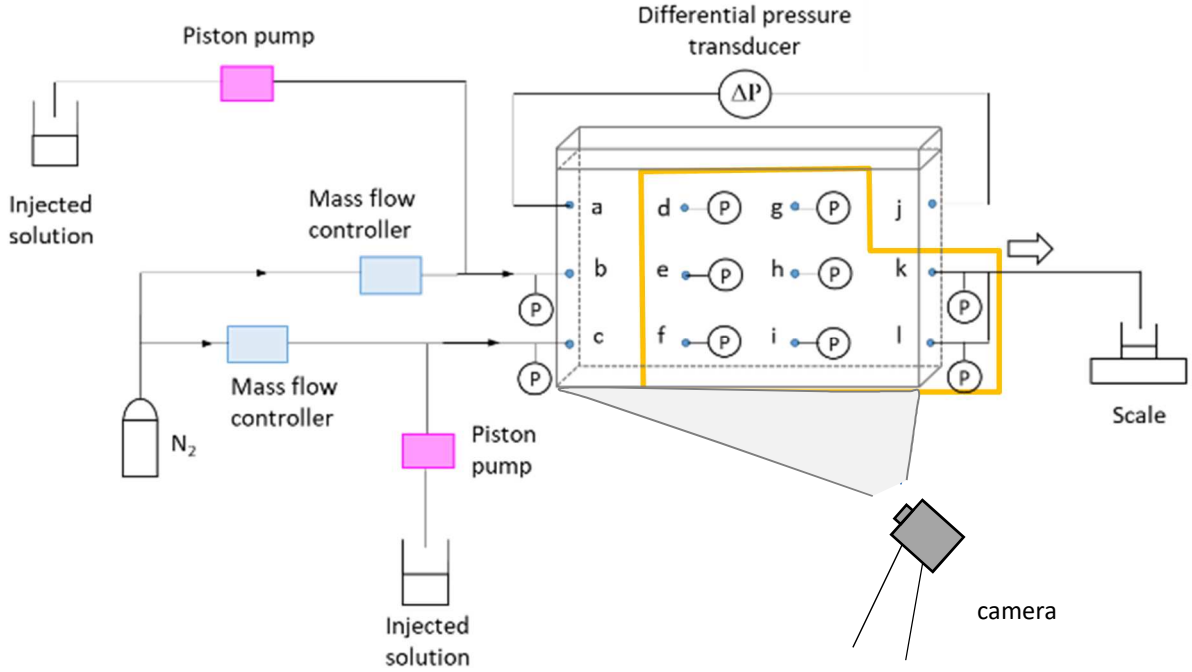

Fig. 1: Schematic representation of the experimental setup for foam injection in 2D porous medium. The pressure taps used to represent pressure maps are contoured in yellow

2.4. Experimental procedure

Experimental tests were designed to investigate different situations that are summarized in Table 1.

Table 1: Summary of experiments

Tests	Purpose	Experimental	Main experimental

		conditions	conditions
Set 1: Foam displacement in a vertical 2D porous medium	Understand foam displacement in a vertical 2D porous medium through its liquid and gaseous phases	Observe a 10×CMC foam front displacement and analyse velocities and pressures	**Experiments without oil**
		Add fluoresceine	
		Inject N_2 in a 10×CMC saturated medium	
Set 2: Influence of surfactant concentration (*Cs*)	Choose the best experimental conditions	Decrease *Cs* to 3.2×CMC	
Set 3: Influence of solid colloidal particles addition	Test foam reinforcement via particles addition	Add 0.5%wt SiO_2 to a 10×CMC foam	
Set 4: Foam displacement in the presence of oil	Understand foam displacement in the presence of oil	Observe a 10×CMC foam front displacement and analyse velocities and pressures	**Experiments with oil**
Set 5: Influence of *Cs* in the presence of oil	Choose the best experimental conditions	Decrease *Cs* to 3.2×CMC	
Set 6: Influence of solid colloidal particles addition	Test foam reinforcement via particles addition in the presence of oil	Add 0.5%wt SiO_2 to a 10×CMC foam	

To understand how foam behaves in a 2D porous medium, and how such behaviour is modified in the presence of an oil layer, two sets of experiments were performed.

A first group of experiments was performed in the absence of oil. The effect of surfactant concentration, injection strategy (gas/liquid co-injection versus Surfactant Alternating Gas (SAG)), and solid particles addition were investigated. The last experiment was performed with a dye added to the foaming solution during the co-injection process.

The second group of experiments was performed in the presence of oil in the upper part of the 2D porous medium. The influence of surfactant concentration and solid particles on foam flow was investigated.

Those experiments are here interpreted and discussed through the pressure measurements and direct visualization of the foam front in the 2D porous media.

2.4.1 Experiments in the absence of oil

The container was filled with sand by gradually introducing sand and water, so that a water saturated porous medium is obtained, with a known porosity and a known pore volume (*PV*). A layer of clay of approximately 15 mm was then added at the top to ensure no-flux boundary conditions. The top of the tank was then closed with a PMMA plug to mechanically tighten it.

To satisfy surfactant adsorption prior to any foam propagation, 3.3 pore volumes of surfactant solution at a concentration *Cs* = 10 × CMC were injected into the water saturated porous medium. This procedure is similar to that early used in 1D column experiments [10].

Gas and foaming solution were then co-injected at a total flow rate Q_{tot} = 24.8 mL.min^{-1}, with a specified quality of 87.5% (volume fraction of gas). These conditions were previously determined from column experiments to be the ones giving the strongest saponin foam [10].

Gas and foaming solution were separately injected through the two taps located at the bottom of the tank (b and c), while opening the two opposite taps to atmospheric pressure. Once injection began, pictures were taken every minute to record the foam front displacement. Moreover, when performing experiments, the mass measurement of the outcoming liquid phase, and pressure values at all taps locations led to the determination of the average water saturation (S_w) of the porous medium:

$$S_w = \frac{V_w}{PV} \quad (1)$$

where V_w is the volume of remaining water, and PV is the total pore volume,

and a local resistance factor, called RF_p, defined as:

$$RF_p = \left[\frac{P_f}{P_w}\right]_{Qtot} \quad (2)$$

where P_f and P_w are respectively the absolute pressure measured for foam and water at the same flow rate and the same location.

For each pressure measurement tap, RF_p represents the increase in pressure due to the flow of foam in the porous medium, and the higher the RF_p, the stronger the foam is. Values were calculated after flow reached steady state for each tap, and a mean RF_p was calculated based on RF_p values throughout the tank.

Because the mean RF_p does not take into account the local pressure charge, absolute pressure values were used to draw 2D pressure maps throughout the tank. The pressure taps used to create those maps are contoured in yellow in Fig. 1.

Influence of surfactant concentration

In order to study the influence of the surfactant concentration (*Cs*), two *Cs* values were chosen as for previous column experiments [10]. One of the experiments was performed with *Cs* = 3.2×CMC, a formulation that has proven to give foam of intermediate strength, and another one was conducted at *Cs* = 10×CMC, which showed a higher foam strength with a higher RF_p.

Surfactant and colloidal particles.

An experiment was carried out, using a 10×CMC saponin foaming solution containing 0.5%wt SiO_2, to see if colloidal particles strengthened foam similarly to what was observed in 1D column experiments [10].

Surfactant Alternating Gas experiment

A surfactant alternating gas (SAG) experiment was carried out to observe the gas phase displacement when injected alone. The aim was to observe whether the liquid phase displacement influenced by any means the gas phase displacement.

To perform the SAG experiment, the porous medium was first saturated with a 10×CMC surfactant solution. Gas alone was then injected at the same total flow rate of Q_{tot} = 24.8 mL.min^{-1} than for other experiments, and pictures taken every minute to record the gas displacement.

Experiments with dyed water

During foam displacement in porous medium, foam can be subject to buoyancy segregation, with part of the gas phase being trapped in pores, while the rest stays mobile. This impacts the

liquid phase displacement during co-injection once the porous medium is filled with foam. In order to dissociate the liquid phase flow from the foam flow, fluorescein was added at 0.05%wt, as a dye to the surfactant solution prior to co-injection. The path taken by the liquid phase could hence be clearly dissociated from the foam flow. Pictures were taken every minute to record the liquid phase displacement.

2.4.2 Experiments in the presence of oil

Experiments of foam propagation in the presence of oil were carried out with a top layer at S_{or} (residual oil saturation), to mimic the sublayer of an oil spread that exists at the interface with an aquifer. By injecting foam via the two lower injection taps (b and c), a strong foam could be generated before it comes in contact with oil.

These tests were done with 2/3 of the tank filled by gradually adding sand and water. In the upper third only, oil was used instead of water. Water was then injected at the top entry, keeping open the opposite exit. When no oil was produced anymore, indicating that S_{or} was reached in that layer, water injection was stopped. After that, 3.3 PV of surfactant solution were injected to saturate the medium before starting co-injection.

Based on visual observation, the instantaneous positions of the foam front were picked-up.

Water saturation and mean RF_p were calculated for each experiment, and measured absolute pressures were used to draw 2D pressure maps.

3. Results and discussion

3.1. Foam propagation in the absence of oil

3.1.1 Influence of surfactant concentration

Pictures taken at a total injected pore volume of 0.28 are displayed in Figure 2, and a plot that represents the time evolution of the foam front propagation is shown in Figure 3.

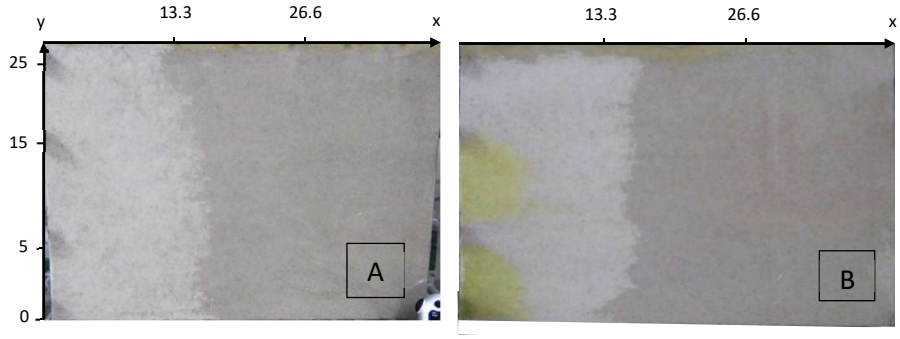

Fig. 2: Foam injection of 3.2×CMC (A), and 10×CMC (B) saponin foam after 0.28 PV injected

Pictures taken during foam displacement with *Cs* = 3.2×CMC and 10×CMC (Fig. 2), show a piston-like front during foam displacement with negligible buoyancy impact. This observation is confirmed in Figure 3 where it can be seen, after the inlet effects, the propagation of a regular and vertical front displacement.

The fact that the front is almost vertical proves that foam is generated wherever gas is present, and that lamellae distribution is even on the full height. In fact, if foam was not formed, only gas propagation would be observed, with quick path through the top of the porous medium. Similarly, a weak foam formation would generate a gradually decreasing density of lamellae on the full height of the container, that may lead to an oblique propagation front.

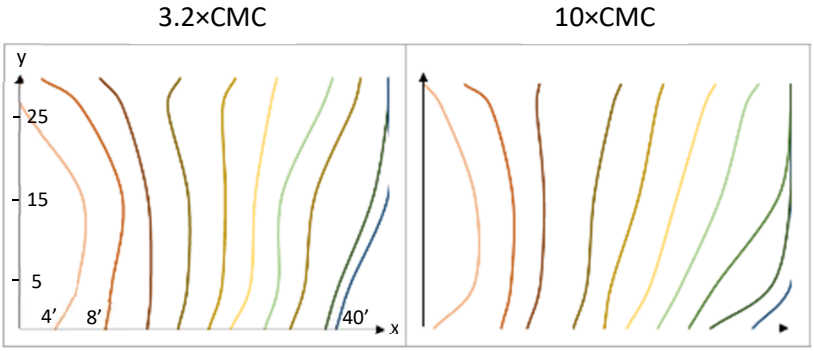

Fig. 3: Front propagation every four minutes at Cs = 3.2xCMC and Cs = 10xCMC

Mean RF_p values, representative of foam strength, are displayed in Table 2. On this table are also reported the ultimate water saturation as deduced from mass balance. At equilibrium state the mean RF_p, is equal to 7.9 for 3.2×CMC, significantly below that corresponding to 10×CMC (9.7), meaning that foam strength does increase with *Cs*. In the meantime, S_w remains stable at 0.36.

Table 2: Mean RF_p and S_w for three different foam formulations in the absence of oil, with and without silica particles

Formulation without oil	3.2×CMC	10×CMC	10×CMC + 0.5%wt SiO_2
Mean RF_p	7.9	9.7	9.9
S_w	0.36	0.35	0.30

Those observations indicate that the foam is so strong that it propagates with a piston-like movement, and that the surfactant concentration has a minor impact on both S_w and the shape of the displacement front, while foam strength is noticeably improved.

3.1.2 Influence of presence of colloidal particles in the foaming solution

Figure 4 represents the picture taken at a total injected pore volume of 0.28 (Figure 4A) and a time evolution of the foam front (Figure 4B).

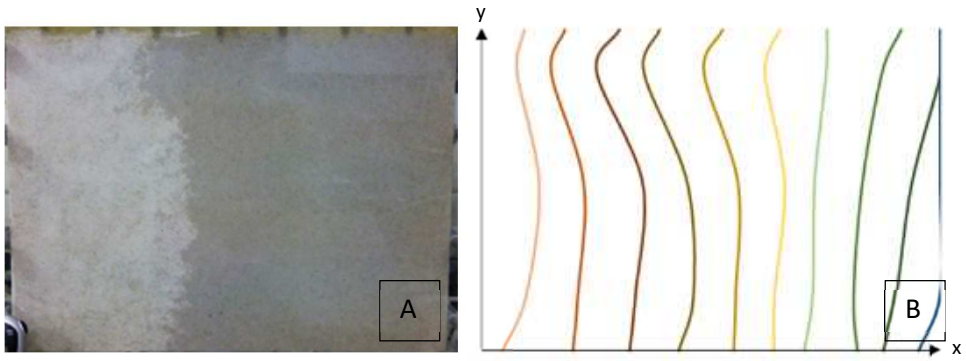

Fig. 4: Foam front after 0.28 PV injected (A) and front position every 4 minutes (B) at Cs = 10×CMC + 0.5%wt SiO_2 saponin foam

The front shape and propagation observed in Figure 4A and B are very similar to the ones observed when foam is generated with surfactant alone. This result confirms that foam is generated wherever gas is present in the porous medium and that the presence of solid particles does not undermine foam generation and propagation.

Considering RF_p, its mean value is equal to 9.9, very close to 9.7 obtained in the absence of particles. On the contrary, the ultimate water saturation S_w decreases from 0.35 to 0.30 (Table 2) when solid colloidal particles are added to the saponin-based formulation, indicating a better sweeping efficiency of the initially water saturated porous medium. In the meantime, a steady piston-like foam front is observed, poorly affected by buoyancy. This decrease of S_w is presumably due to the formation of more rigid lamellae, as solid colloid adsorption at the liquid-gas interface generates lamellae that are more resistant to drainage. Thus, a slightly higher RF_p is observed.

3.1.3 Comparison between liquid/gas co-injection and SAG

Figure 5 presents a picture of the foam front displacement taken at total pore volume injected of 0.27PV when gas is injected in a porous medium that was beforehand saturated by the foaming solution at *Cs* = 10×CMC.

Fig. 5: N_2 injection in a Cs = 10×CMC surfactant saturated porous medium after 0.27 PV injected

A comparison with the previous figures shows that the front propagation is almost vertical and is very similar to that previously obtained during co-injection. This proves that foam is generated wherever gas and foaming solution are present in the porous medium and does not depend on the injection process.

3.1.4 Injection of dyed foaming solution

To characterize the specific path taken by water and gas, an experiment was performed with dyed water. Similarly to the other experiments, the porous medium was first saturated with aqueous solution to satisfy surfactant adsorption. A foaming solution was then dyed by adding fluorescein and co-injection was performed under the same conditions as before. The path of the newly injected solution could then be followed as it appears in yellow in Figure 2B and Figure 6 after injection of respectively 0.28 and 2.4 *PV*.

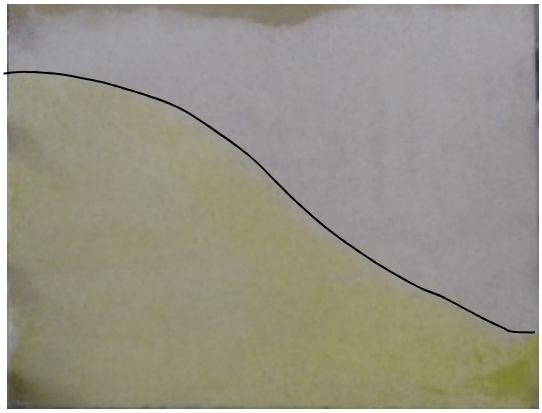

Fig. 6: Injection of a 10×CMC foam with a coloured liquid phase after 2.4 PV injected

In Figure 6, two zones with different colours are observed. Gas and aqueous dyed solution are co-injected at a given value of foam quality and, after 2.4 *PV* of total fluid injected, the entire tank is saturated with foam. However, a colour difference can be observed from top to bottom, which establishes the presence of a vertical foam quality stratification. The aqueous foaming solution in yellow is moving down slowly while gas is moving up without preventing foam formation and propagation in the porous medium.

This behaviour can be explained in the following way. Literature results shows [22] that as gas fraction increases, the apparent viscosity and capillary pressure P_c increase until they reach a maximum value at f^*_g. At that critical gas fraction, the apparent viscosity is maximum and P_c reaches its ultimate value P^*_c. Below f^*_g, foam is in the low quality regime: gas is discontinuous and trapped in a lamellae network. The pressure drop is independent of the gas velocity and depends on the liquid velocity. In contrast, for $f_g > f^*_g$ foam is in the high quality regime, where the pressure drop is dependent of the gas velocity and independent of the liquid velocity. For gas fraction well above f^*_g, the occurrence of bubbles coalescence increases drastically, leading to an increase in gas mobility and a decrease in the apparent viscosity. Consequently, in the vicinity of f^*_g, a given apparent viscosity may correspond to two f_g values: one of them > f^*_g and the other < f^*_g.

In those experiments, nitrogen and the foaming solution were co-injected at f_g = 87.5%, which was previously determined as being close to f^*_g [10]. However, in 2D experiments, due to the impact of buoyancy, the local gas fraction should span from lower quality in the bottom of the container to higher quality at the top. Moreover, the change of pressure with height is low (Figure 7), and results are consistent; foam quality is higher at the top, and the pressure drop is almost independent of the liquid phase velocity.

In other words, based on the water mobility map (Figure 6), a small spatial variation of S_w can largely impact the relative permeability to water k_{rw} [23] leading to an easier water flow in the lower part. In the meantime, the S_w gradient has little impact on the relative permeability to gas k_{rg}, thus explaining why the front displacement is almost vertical, and why the f_g gradient has a limited impact on the velocity height dependency. This specific study indeed corroborates the spatial variation observed of both velocity front displacement and resistance factor.

3.1.5 Pressure drop analysis

The behavior of foam generation and propagation in 2D porous media can be analyzed considering the absolute pressure measurements P_f and P_w at each pressure tap during co-injection. However, and for convenience, the study was restricted to pressure taps located at d, e and f measurement points (See Fig. 1), to follow foam displacement at three different heights (5, 15 and 25 cm). Thereby, the resistance factor RF_p is plotted versus the injected pore volume

(corresponding to time) in Figure 7, for such a bottom, middle and top positions. Foaming conditions are the same as in Figure 2.

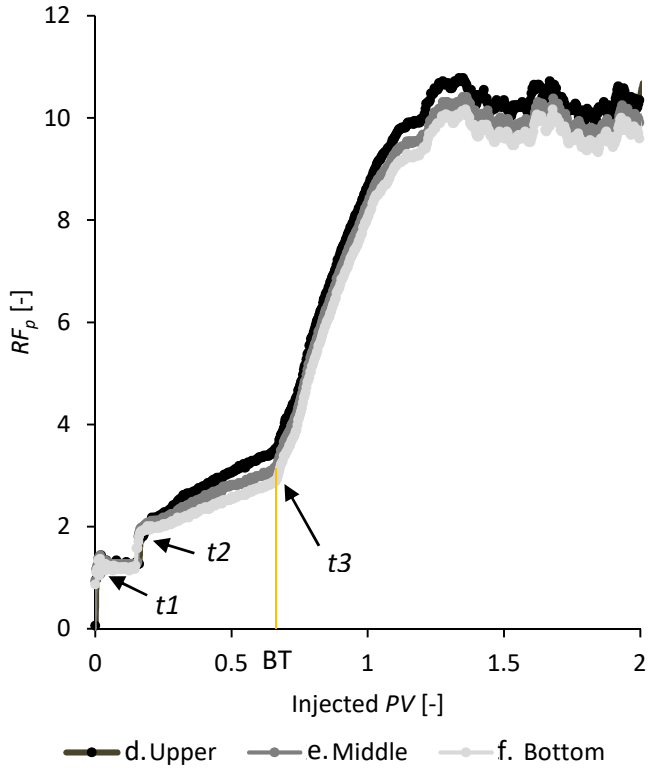

Fig. 7: Pressure variations at the 13.3 cm right of the tank for a foam formulation of 10×CMC with varying heights of 5 cm (Bottom), 15 cm (Middle) and 25 cm (Upper). Breakthrough (BT) location is indicated by a vertical line

Once co-injection begins at $t = t_1$, a sudden increase is observed as aqueous solution flows at that location. Between t_1 and t_2, the plateau value equals unity as only water is flowing. At $t = t_2$, the pressure suddenly increases once foam reaches the pressure taps. Then, between t_2 and t_3 foam steadily propagates within the porous medium and pressure linearly increases as a function of the injected volume, in a similar way to what was observed in 1D column experiments [10]. At $t = t_3$, foam breakthrough (*BT*) is observed while pressure keeps increasing.

This behaviour is in apparent contrast with what is usually observed in column experiments where pressure quickly stabilized after the breakthrough. In a previously published work, Portois *et al.* [23] have noted that when a pre-generated foam is injected in a porous medium initially containing a surfactant-free water, 8 *PV* beyond the *BT* were necessary to reach a steady state. They attributed this delay to surfactant adsorption. However, such an explanation cannot hold here because the porous medium was saturated with surfactant prior to nitrogen/foaming solution co-injection.

A possible explanation is that when foam locally breaks through, pressure at the corresponding exit point suddenly increases from water pressure to foam pressure. As a consequence, and to maintain the flow regime in the container, the pressure at taps d, e and f increases, keeping constant the pressure drop. This process continues until both exiting sides of the container are filled with foam, which is when the injected volume is around 1.2 *PV*.

In the last step, the pressure level is nearly stabilized, showing a new plateau that reflects the equilibrium between the lamella creation rate and its destruction, probably due to strong capillary pressure, high drainage and coalescence.

Experimental data (Figure 7) also show that the local pressure slowly increases from the bottom to the top of the tank. This indicates a slight foam weakening with height, as suggested

by the small change in the velocity front (Figure 4B), although one must keep in mind that when gas fraction fluctuates around f^*_g, the local viscosity is only moderately changed.

3.2. Foam propagation in the presence of oil

In the previous section, foam formation and propagation were investigated in a 2D porous media for different formulations, by focusing on the resistance factor and propagation front. However, and for application purposes, the aim of the present study was to investigate how foam behaves when it comes in contact with oil. To this end, the previous experiments have been repeated with an upper layer of the porous medium now containing oil at residual saturation (S_{or}). It is worth noting that, similarly to the previous experiments, the upper exit point was closed. First, the influence of saponin concentration on the foam front displacement and resistance factor were investigated, before considering the effect of the addition of SiO_2 solid colloids.

In the first experiment, a 3.2×CMC based foam was injected in a porous medium saturated with surfactant, with a top layer at S_{or}. Foam quality and total flow rate were the same as used for experiments in the absence of oil. Such experiment was then repeated for concentrations of 10×CMC of saponin and 10×CMC saponin + 0.5%wt SiO_2. Pictures taken after co-injection of 0.27

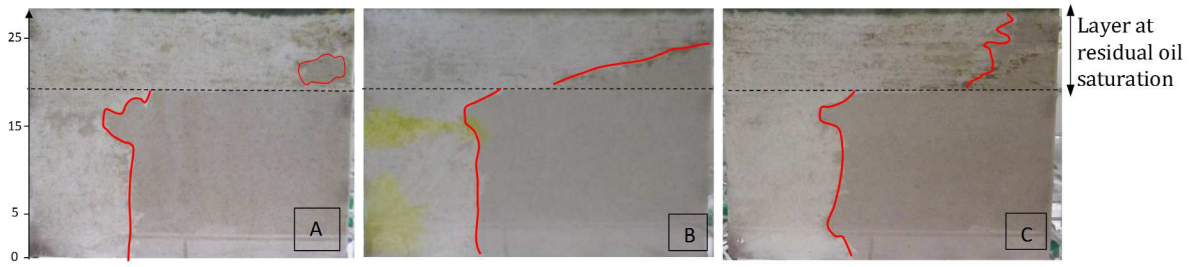

Fig. 8: Saponin foam in the presence of oil after 0.27 PV injected. Injection of 3.2×CMC (A), 10×CMC (B) and 10×CMC + 0.5%wt SiO_2 (C)

PV are displayed on Figure 8 for each formulation, and call for some preliminary remarks:

- Below the oily layer, the foam displacement front is almost vertical whatever the formulation, with small fluctuations in the transverse direction.
- For 3.2×CMC of saponin (Figure 8A), a fast foam destruction is observed when it comes in contact with oil. Then, a 3D connected gaseous phase forms and gas breakthrough happens shortly after, with an apparent fingering effect, and a mean velocity much higher than in the rest of the container.
- For 10×CMC of saponin (Figure 8B), the displacement front in the oily zone is more stable than for low saponin concentration, even if oil-induced destruction through bubble coalescence can still be observed. As a consequence, a partial phase segregation occurs, arising in a local oblique displacement front with a mean velocity in the top layer more than twice the mean velocity in the bottom layer.
- For 10×CMC of saponin+ 0.5%wt SiO_2 (Figure 8C), the oily layer is more efficiently swept and the displacement front is straightened. This brings out that SiO_2 particles effectively act as a damping agent against oil-induced bubble coalescence. As recalled, in the absence of oil, SiO_2 addition moderately contributes to foam strengthening and mainly contributes to foam stabilisation in the presence of oil. These foams, usually termed as Pickering-like foams are then less brittle and have a higher resistance to oil-induced destruction.

It should be noted that for all these experiments, no noticeable oil was produced during co-injection, and that S_{or} was nearly constant over time.

Besides these visual observations, water saturation S_w, as well as the local resistance factor RF_p were continuously determined during co-injection. In the present situation, some of the pressure sensors were located in the oil-free layer, and others in the oily layer. To illustrate the general features observed, Figure 9 shows the RF_p variations as a function of the total injected volume for a foaming solution that contains 10×CMC saponin. The RF_p data correspond to the oil-free zone through the pressure measurements at locations e, f and in the oily layer through the pressure measurement at location d (see Figure 1). Regardless of the absolute values of RF_p, the RF_p vs PV curves in the oil-free part of the container are quite similar to those already obtained in the absence of oil.

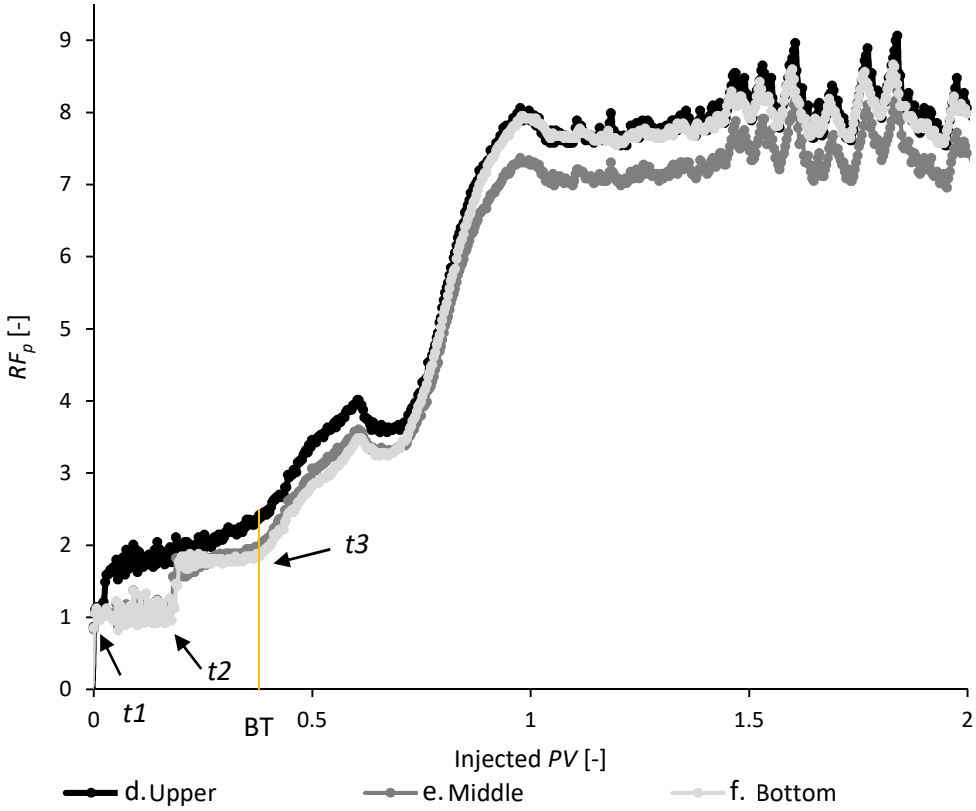

Fig. 9: RF_p variations at 13.3 cm right for a foam formulation of 10×CMC in the presence of oil. Breakthrough (BT) is represented by the yellow line

However, in the oily domain, the curve significantly changes especially before gas breakthrough. As the co-injection process begins, the pressure increases after a very short plateau regime while such a plateau holds in the oil-free zone until $t = t_2$. In fact, in the oily part of the container, when foam comes in contact with oil, some coalescence events occur and foam partially loses its structure and becomes weaker. Consequently, the lamellae density decreases and continuous gaseous channels are formed where gas quickly propagates. After gas breakthrough (BT), all pressure signals change in a similar way. But because the upper exit tap j is turned off, it is difficult to quantitatively compare visual observations with the RF_p versus PV curves.

However, to get an overall idea on how these formulations behave in the presence of oil, the average of ultimate RF_p values from the entire container can be compared. These data are given on Table 3, where both water saturation and the initial S_{or} in the top layer are also given. Firstly, whatever the formulation, the average RF_p values are lower in the presence of oil (Table 3): a consequence of the loss of foam structure due to the defoaming contribution of oil. Such a loss is

more remarkable in the case of 3.2×CMC saponin, and is significantly less pronounced for other formulations. Secondly, a velocity ratio "*Vr*" can be calculated by time averaging the front velocity in the top layer "V_{tot}" divided by that corresponding to oil-free zone before gas breakthrough "V_{bottom}":

$$Vr = \frac{V_{tot}}{V_{bottom}} \qquad (3)$$

These data are also given in Table 3. The velocity ratio is well above unity whatever the formulation due to the oil defoaming nature, and this is more pronounced for 3.2×CMC for which foam is largely weakened in presence of oil. For higher saponin content, *Vr* ratio noticeably decreases, and such a decrease is even more pronounced when SiO_2 particles are added to the foaming solution. Besides, by considering S_w, the remaining water saturations are indeed higher than those previously obtained in the absence of oil.

Table 3: Mean RF_p, S_w, S_{or} and Vr for three different foam formulations with and without silica particles, in the presence of oil

Formulation with oil	3.2×CMC	10×CMC	10×CMC + 0.5%wt SiO_2
Mean RF_p	2.2	8.0	7.8
S_w	0.43	0.41	0.42
S_{or}	0.023	0.022	0.020
Vr	4.03	2.74	2.59

Otherwise it is more telling by considering pressure maps drawn by using pressures measured at steady state. To that end, such pressure maps are displayed in Figure 10 for the three formulations and for the two kinds of experiments.

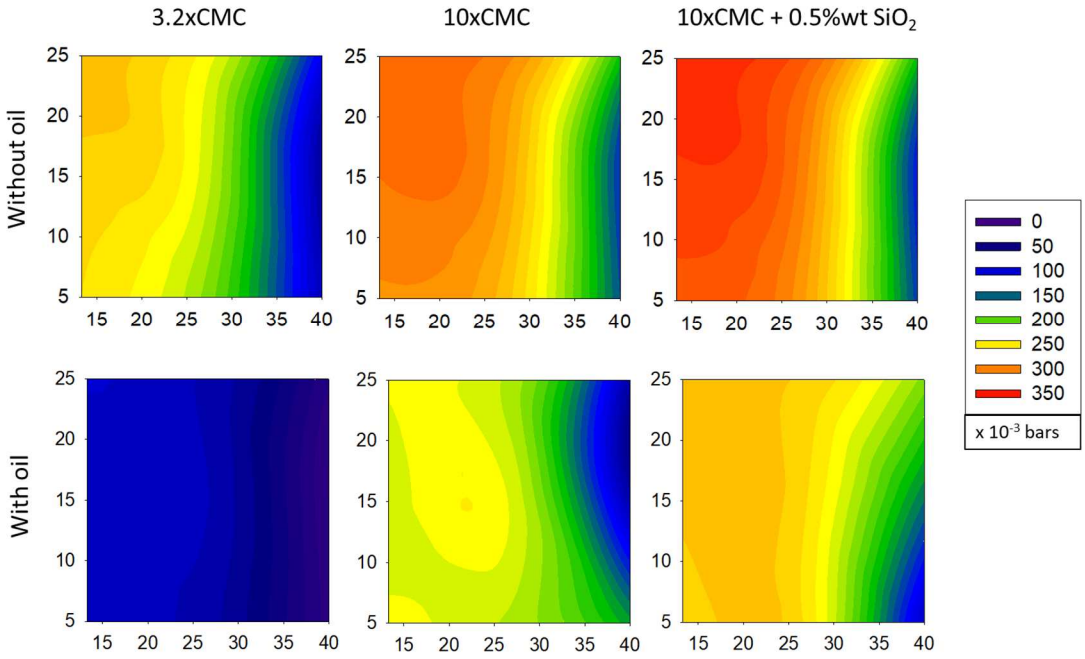

Fig. 10: Pressure maps at equilibrium for different foam formulations obtained with oil and without oil

It may be seen therefore that the increase in saponin and SiO_2 concentrations makes foam stronger, and that in the presence of oil, foam becomes weaker. However, the use of solid colloids such as silica particles appears to be a way to stem foam destruction by oil, as pressures are higher than in the case of silica-free formulations, and present as vertical fronts.

It appears that the presence of foam in the system not only allows a full sweeping of the porous medium, but also has a blocking effect on the full height of the tank, even in the presence of residual oil.

Thus, the suggested mechanism for foam propagation is the following: as gas and foaming solution starts invading the lower part of the porous medium, foam is created and starts propagating. Then, as foam reaches the upper layer containing oil, it is partly destroyed and locally generates a higher relative permeability to gas. It thus facilitates flow with a preferential path, visualized by a high front velocity. The increase in velocity in the top of the tank leads to an increased pressure. As gas and surfactant solution are injected into the porous medium, foam strengthens in the top layer and given the right formulation, a vertical front can be observed.

Meanwhile in the bottom layer, foam propagates with a lower velocity. It is slightly affected by the presence of oil in the top layer, because some gas is deviated to the top layer, implying that foam quality may drop below 87.5% in the bottom layer. As foam keeps propagating, pressure gradually reaches equilibrium, and after a few *PV*, stabilization is reached. Foam entirely fills the porous medium with homogeneous pressures on the full height, showing the foam ability to entirely block the porous medium, even in areas initially at S_{or}.

4. Conclusion

First, it is worth remembering that the goal of the present study was to investigate how the presence of oil impacts foam formation during a liquid-gas co-injection process. Literature and previous experiments have shown that organic phases, such as LNAPL, usually act as defoaming agents that thwart the use of foam in remediation treatments. So, the focus was here put on obtaining a strong foam that undergoes minimum buoyancy effects and is significantly resistant to oil. To meet these requirements, the synergy between a biological surfactant (saponin) and silica colloidal particles was explored to obtain a strong and stable foam. In the investigations,

gas-liquid co-injection experiments were carried out in a large size 2D porous medium in the absence and in the presence of oil.

When no oil is present, even under circumstances of high foam quality and optimum total flow rate, foam displacement is not trivial. Albeit foam visually sweeps the porous medium in a piston-like way, buoyancy segregation still acts, and a gas/liquid saturation gradient takes place across the flow direction. The corresponding local resistance factor, instantaneous velocity and water saturation values are consistent with each other. This observed behaviour was coherent with the variation of foam quality across the container and with the impact of such a variation on foam viscosity, taking into account that the injected gas fraction was close to its critical value f^*_g. As the surfactant concentration increases, foam strengthens due to a higher lamellae stability that prevents bubbles to coalesce. If SiO_2 colloidal particles are incorporated in the formulation, the resistance factor is slightly enhanced and S_w is substantially decreased. This may be summarized by saying that SiO_2 addition probably arises in thicker lamellae without significantly affecting the foam structure, and bubbles are in a shield consisting of solid SiO_2 colloidal particles.

By repeating the experiment in the presence of a layer initially at residual oil saturation, formed foams are destroyed when they come in contact with oil, thus increasing the local gas mobility while it seems unaffected in the rest of the container. However, foam resistance to oil-induced destruction is less damaging when the surfactant concentration increases, and is damped when SiO_2 particles are added to the formulation.

Finally, it should be reminded that the co-injection process is restricted to medium permeability porous media, and that foam pre-generation is indicated in case of highly permeable porous media [24, 25]. Moreover, after bubble generation, solid colloids can adsorb at the gas-liquid interface due to their slow diffusion besides the significant energy intake needed for particles adsorption. So, the process efficiency is multifactorial and depends, among other things, on the characteristics of the porous medium, the oil composition, the nature of the foaming solution and the gas and aqueous solution injection rates. Those characteristics should hence be studied and taken into account before using the technique on the field.

Acknowledgments

This research was founded by InnovaSol Consortium. We thank Marian Momtbrun for assistance in conducting experiments.

References

[1] G.J. Hirasaki, C.A. Miller, R. Szafranski, J.B. Lawson, N. Akiya, Surfactant/Foam Process for Aquifer Remediation, in: International Symposium on Oilfield Chemistry, Society of Petroleum Engineers, Houston, Texas, 1997. https://doi.org/10.2118/37257-MS.

[2] O.G. Apaydin, A.R. Kovscek, Surfactant Concentration and End Effects on Foam Flow in Porous Media, Transport in Porous Media. 43 (2001) 511–536. https://doi.org/10.1023/A:1010740811277.

[3] H.J. Bertin, O.G. Apaydin, L.M. Castanier, A.R. Kovscek, Foam Flow in Heterogeneous Porous Media: Effect of Cross Flow, SPE Journal. 4 (1999) 75–82. https://doi.org/10.2118/56009-PA.

[4] A.R. Kovscek, H.J. Bertin, Foam Mobility in Heterogeneous Porous Media, Transport in Porous Media. 52 (2003) 17–35. https://doi.org/10.1023/A:1022312225868.

[5] H. Bertin, E.D.C. Estrada, O. Atteia, Foam placement for soil remediation, Environ. Chem. 14 (2017) 338–343. https://doi.org/10.1071/EN17003.

[6] X. Shen, L. Zhao, Y. Ding, B. Liu, H. Zeng, L. Zhong, X. Li, Foam, a promising vehicle to deliver nanoparticles for vadose zone remediation, Journal of Hazardous Materials. 186 (2011) 1773–1780. https://doi.org/10.1016/j.jhazmat.2010.12.071.
[7] C. Portois, E. Essouayed, M.D. Annable, N. Guiserix, A. Joubert, O. Atteia, Field demonstration of foam injection to confine a chlorinated solvent source zone, Journal of Contaminant Hydrology. 214 (2018) 16–23. https://doi.org/10.1016/j.jconhyd.2018.04.003.
[8] M.M. Almajid, A.R. Kovscek, Pore-level mechanics of foam generation and coalescence in the presence of oil, Adv Colloid Interface Sci. 233 (2016) 65–82. https://doi.org/10.1016/j.cis.2015.10.008.
[9] R. Farajzadeh, A. Andrianov, R. Krastev, G.J. Hirasaki, W.R. Rossen, Foam-oil interaction in porous media: implications for foam assisted enhanced oil recovery, Adv Colloid Interface Sci. 183–184 (2012) 1–13. https://doi.org/10.1016/j.cis.2012.07.002.
[10] N. Forey, O. Atteia, A. Omari, H. Bertin, Saponin foam for soil remediation: On the use of polymer or solid particles to enhance foam resistance against oil, Journal of Contaminant Hydrology. 228 (2020) 103560. https://doi.org/10.1016/j.jconhyd.2019.103560.
[11] S.I. Karakashev, O. Ozdemir, M.A. Hampton, A.V. Nguyen, Formation and stability of foams stabilized by fine particles with similar size, contact angle and different shapes, Colloids and Surfaces A: Physicochemical and Engineering Aspects. 382 (2011) 132–138. https://doi.org/10.1016/j.colsurfa.2010.09.023.
[12] Q. Sun, Z. Li, S. Li, L. Jiang, J. Wang, P. Wang, Utilization of Surfactant-Stabilized Foam for Enhanced Oil Recovery by Adding Nanoparticles, Energy Fuels. 28 (2014) 2384–2394. https://doi.org/10.1021/ef402453b.
[13] B.P. Binks, T.S. Horozov, Aqueous Foams Stabilized Solely by Silica Nanoparticles, Angewandte Chemie International Edition. 44 (2005) 3722–3725. https://doi.org/10.1002/anie.200462470.
[14] E. Dickinson, Food emulsions and foams: Stabilization by particles, Current Opinion in Colloid & Interface Science. 15 (2010) 40–49. https://doi.org/10.1016/j.cocis.2009.11.001.
[15] M. Longpré-Girard, R. Martel, T. Robert, R. Lefebvre, J.-M. Lauzon, 2D sandbox experiments of surfactant foams for mobility control and enhanced LNAPL recovery in layered soils, J. Contam. Hydrol. 193 (2016) 63–73. https://doi.org/10.1016/j.jconhyd.2016.09.001.
[16] I. Bouzid, J. Maire, S.I. Ahmed, N. Fatin-Rouge, Enhanced remedial reagents delivery in unsaturated anisotropic soils using surfactant foam, Chemosphere. 210 (2018) 977–986. https://doi.org/10.1016/j.chemosphere.2018.07.081.
[17] R. Singh, K.K. Mohanty, Foam flow in a layered, heterogeneous porous medium: A visualization study, Fuel. 197 (2017) 58–69. https://doi.org/10.1016/j.fuel.2017.02.019.
[18] Y.-J. Tsai, F.-C. Chou, S.-J. Cheng, Using tracer technique to study the flow behavior of surfactant foam, Journal of Hazardous Materials. 166 (2009) 1232–1237. https://doi.org/10.1016/j.jhazmat.2008.12.038.
[19] A. Pradhan, A. Bhattacharyya, Quest for an eco-friendly alternative surfactant: Surface and foam characteristics of natural surfactants, Journal of Cleaner Production. 150 (2017) 127–134. https://doi.org/10.1016/j.jclepro.2017.03.013.
[20] C.N. Mulligan, Recent advances in the environmental applications of biosurfactants, Current Opinion in Colloid & Interface Science. 14 (2009) 372–378. https://doi.org/10.1016/j.cocis.2009.06.005.
[21] G. Orts-Gil, K. Natte, D. Drescher, H. Bresch, A. Mantion, J. Kneipp, W. Österle, Characterisation of silica nanoparticles prior to in vitro studies: from primary particles to agglomerates, J Nanopart Res. 13 (2011) 1593–1604. https://doi.org/10.1007/s11051-010-9910-9.
[22] Z.I. Khatib, G.J. Hirasaki, A.H. Falls, Effects of Capillary Pressure on Coalescence and Phase Mobilities in Foams Flowing Through Porous Media, SPE Reservoir Engineering. 3 (1988) 919–926. https://doi.org/10.2118/15442-PA.

557 [23] C. Portois, C.S. Boeije, H.J. Bertin, O. Atteia, Foam for Environmental Remediation:
558 Generation and Blocking Effect, Transp Porous Med. 124 (2018) 787–801.
559 https://doi.org/10.1007/s11242-018-1097-z.
560 [24] J. Maire, E. Brunol, N. Fatin-Rouge, Shear-thinning fluids for gravity and anisotropy
561 mitigation during soil remediation in the vadose zone, Chemosphere. 197 (2018) 661–669.
562 https://doi.org/10.1016/j.chemosphere.2018.01.101.
563 [25] R. Aranda, H. Davarzani, S. Colombano, F. Laurent H. Bertin, Experimental study of foam
564 flow in highly permeable porous media for soil remediation, Transport in Porous Media
565 (2020) Doi.org/10.1007/s11242-020-01443,

566